



This discussion paper is/has been under review for the journal Hydrology and Earth System Sciences (HESS). Please refer to the corresponding final paper in HESS if available.

A new approach to accurate validation

C. Sun et al.

A new approach to accurate validation of remote sensing retrieval of evapotranspiration based on data fusion

C. Sun, D. Jiang, J. Wang, and Y. Zhu

Institute of Geographical Sciences and Natural Resources Research, CAS, Beijing, China

Received: 12 February 2010 – Accepted: 24 February 2010 – Published: 3 March 2010

Correspondence to: D. Jiang (jiangd@lreis.ac.cn)

Published by Copernicus Publications on behalf of the European Geosciences Union.

Title Page

Abstract

Introduction

Conclusions

References

Tables

Figures

◀

▶

◀

▶

Back

Close

Full Screen / Esc

Printer-friendly Version

Interactive Discussion



Abstract

The study presented a new method of validating the remote-sensing (RS) retrieval of evapotranspiration (ET) under the support of a distributed hydrological model: Soil and Water Assessment Tool (SWAT). In this method, the output runoff data based on a fusion of ET data, meteorological data and rainfall data, etc. were compared with the observed runoff data, so as to carry out validation analysis. A new pattern of validating the ET data obtained from RS retrieval, which was more appropriate than the conventional means of observing the ET at several limited stations based on eddy covariance, was proposed. It has integrated the advantage of high requirement of ET with high spatial resolution in the distributed hydrological model and that of the capacity of providing ET with high spatial resolution in RS methods.

First, the ET data in five years (2000–2004) were retrieved with RS according to the principle of energy balance. The temporal/spatial distribution of monthly ET data and related causes were analyzed in the year of 2000, and the monthly ET in the five years was calculated according to the PM model. Subsequently, the results of the RS retrieval of ET and the PM-based ET calculation were compared and validated. Finally, the ET data obtained from RS retrieval was evaluated with the new method, under the support of SWAT, meteorologic data, Digital Elevation Model (DEM), landuse data and soil data, etc. as the input, being compared with the PM-based ET.

According to the ET data analysis, it can be inferred that the ET obtained from RS retrieval was more continuous and stable with less saltation, while the PM-based ET presented saltation, especially in the year of 2000 and 2001. The correlation coefficient between the monthly ET in two methods reaches 0.8914, which could be explained by the influence from clouds and the inadequate representativeness of the meteorologic stations. Moreover, the PM-based ET was smaller than the ET obtained from RS retrieval, which was in accordance with previous studies (Jamieson, 1982; Dugas and Ainsworth, 1985; Benson et al., 1992; Pereira and Nova, 1992).

A new approach to accurate validation

C. Sun et al.

[Title Page](#)

[Abstract](#)

[Introduction](#)

[Conclusions](#)

[References](#)

[Tables](#)

[Figures](#)

◀

▶

◀

▶

[Back](#)

[Close](#)

[Full Screen / Esc](#)

[Printer-friendly Version](#)

[Interactive Discussion](#)



After the data fusion, the correlation ($R^2=0.8516$) between the monthly runoff obtained from the simulation based on ET retrieval and the observed data was higher than that ($R^2=0.8411$) between the data obtained from the PM-based ET simulation and the observed data. As for the RMSE, the result (RMSE=26.0860) between the simulated runoff based on ET retrieval and the observed data was also superior to the result (RMSE=35.71904) between the simulated runoff obtained with PM-based ET and the observed data. As for the MBE parameter, the result (MBE=−8.6578) for the RS retrieval method was obviously better than that (MBE=−22.7313) for the PM-based method. The comparison of them showed that the RS retrieval had better adaptivity and higher accuracy than the PM-based method, and the new approach based on data fusion and the distributed hydrological model was feasible, reliable and worth being studied further.

1 Introduction

Evapotranspiration (ET), including the evaporation from soil surface and the vegetation transpiration, is a major component in the water and heat balance of terrestrial ecosystems as well as in the water, energy and carbon cycles on the Earth's surface (Hussey and Odum, 1992; Garatuza-Payan and Watts, 1998; Drexler et al., 2004; Parasuraman et al., 2007; Gao and Long, 2008; Zhou and Zhou, 2009).

Various ET studies have been conducted in many regions throughout the world on the basis of meteorologic data (Mohan, 1991; Amatya et al., 1995; Boegh et al., 2002, 2009; George et al., 2002; DehghaniSanj et al., 2004; Garcia et al., 2004) with several main ET equations and corresponding input data. For daily ET calculation, the PM method requires the daily data, including the maximum and the minimum air temperature (T_{\max} and T_{\min}), the Relative Humidity (RH), the Solar Radiation (RS) and the Wind Speed (u), as the input. The Priestley-taylor (PT) method also requires multiple climate parameters to estimate ET, while the Hargreaves (HG) equation (Hargreaves and Samani, 1982) requires air temperature data to estimate ET. It seems that the selection

A new approach to accurate validation

C. Sun et al.

[Title Page](#)

[Abstract](#)

[Introduction](#)

[Conclusions](#)

[References](#)

[Tables](#)

[Figures](#)

◀

▶

◀

▶

[Back](#)

[Close](#)

[Full Screen / Esc](#)

[Printer-friendly Version](#)

[Interactive Discussion](#)



of a proper method for any station and/or area depends on many factors such as the climate condition, the accessibility of data needed, the complexity of method, time and cost. Although one version of the PM method has been established as the standard for calculating ET (Allen et al., 1998), related studies implied that none of the ET estimation methods was applicable at all times and different stations (Yagob, 2006).
5

Since 1980s, energy balance methods have been regarded as the preferred method for estimating the wide-area ET in the RS field (Overgaard et al., 2006), and numerous physical and empirical RS-based models have been developed for ET estimation in many different fields (Granger, 1995, 1997, 2000; Bastiaanssen et al., 1998a, b; Bastiaanssen, 2000; Su, 2002; Jacob et al., 2002b; Allen et al., 2005; Wang et al., 2005; Neale et al., 2005; Garatuza et Watt, 2005; Batra et al., 2006). Most of RS methods for estimating ET are based wholly or partially on the energy balance principle, with net radiation adopted as the principal driving parameter (Jabloun and Sahli, 2008), which has led to a breakthrough in the high-resolution ET acquisition.
10

Unfortunately, it is still a difficult problem to validate the ET data obtained with RS retrieval independently (Kite and Droogers, 2000). The conventional means of accessing retrieval results using observed ET data, including the Large Aperture Scintillometer (Jiang et al., 2003; Wang and Jiang, 2005) and the eddy covariance method (Kustas and Norman, 1999; Kite and Droogers, 2000; Wei et al., 2006; Sun and Song, 2008; Boegh et al., 2009; Zhou and Zhou, 2009; Teresa et al., 2009; Heilman et al., 2009; Guan and Wilson, 2009), have their limitations, because the observed data are based on one or several stations (Kite and Droogers, 2000; Gavila'n et al., 2006; Jabloun and Sahli, 2008; Liu et al., 2010), which are rather limited in amount even in developed countries. Additionally, the assumption that field methods are probably the most reliable is hard to justify, because different field methods differ considerably (Kite and Droogers, 2000). Moreover, validating the RS retrieval results with the ET model to calculate ET (Kite and Droogers, 2000) involves the same problem, for the meteorological data on which the ET model is based are basically observable just in several limited stations, and the differences among different algorithms should also be considered.
20
25

A new approach to accurate validation

C. Sun et al.

[Title Page](#)[Abstract](#)[Introduction](#)[Conclusions](#)[References](#)[Tables](#)[Figures](#)[◀](#)[▶](#)[◀](#)[▶](#)[Back](#)[Close](#)[Full Screen / Esc](#)[Printer-friendly Version](#)[Interactive Discussion](#)

Accordingly, it is urgent to find a proper method to validate accurately the ET data obtained from RS retrieval with high resolution. With the emergence and rapid development of distributed hydrological models, it has become urgent to adopt high-resolution ET data as the input and the measurable runoff data as the output, which provides a possibility for validating the ET obtained from RS retrieval using a distributed hydrological model. This study presents a data fusion method for the validation of RS retrieval of ET based on distributed hydrological model. In the method, the runoff, which can be observed accurately, is adopted as one of the main analysis parameters. Among the advanced distributed hydrological models, SWAT has been widely used around the world, and some related researches on the calibration and sensitivity (Kannan et al., 2007a; Immerzeel and Droogers, 2008) as well as the climate change sensitivity have already existed (Fichlin et al., 2009). Hereby, SWAT was adopted as the fusion model in this study.

Therefore, the objectives of this study were to: (1) establish a data fusion pattern to validate the RS retrieval of ET; (2) compare the monthly ET obtained based on Penman-Monteith, which has been established as a standard for calculating ET (Allen et al., 1998), with the RS result, so as to evaluate the ET results obtained from RS retrieval preliminarily; (3) validate the ET results based on RS retrieval by comparing with that based on the PM model using SWAT with the new pattern and the observed data of the runoff, aiming at validating an effective mode to validate the RS retrieval of ET.

2 Study area and data description

2.1 Study area

Zhelin Basin, the study area, is located in the upper and middle reaches of the Xiuhe River Basin in the Northeast Jiangxi province, China. It is one of the branches of the Yangtze River, with the Zhelin Reservoir in its lower reaches, which is located in

A new approach to accurate validation

C. Sun et al.

[Title Page](#)

[Abstract](#)

[Introduction](#)

[Conclusions](#)

[References](#)

[Tables](#)

[Figures](#)

◀

▶

◀

▶

[Back](#)

[Close](#)

[Full Screen / Esc](#)

[Printer-friendly Version](#)

[Interactive Discussion](#)



east longitude 115.5° and north latitude 29.2° . The Zhelin Basin is in a strip shape, i.e., about 176 km from west to east and more than 84 km from south to north on average, with the altitudes within the range of 10–1200 m. The area of basin is about 9340 km^2 , and the main river is about 353 km long with bending coefficient of 1.69.

5 The basin is surrounded by mountains on three sides, i.e., the Mufu Mountains in the north, the Dawei Mountains in the west and the Jiuling Mountains in the south. In this way, a closed watershed is formed. The land type composition of the basin is: 60 percent of mountains, 30 percent of hills, 7 percent of hillocks and the rest 3 percent of valley plains. Figure 1 shows the location and the geomorphologies, etc. of the study

10 area. The basin contains abundant ground vegetation, with dense forests full of firs and pines. Only in the middle reaches, scanty bald hills can be found, while sparse grassland is distributed in a few regions in the lower reaches. The soil in the basin is loose.

Belonging to the Asian southeast monsoon climate area, the Zhelin Basin is one of 15 the five rainstorm centers of Jiangxi province, China, with the mean annual rainfall of 1597.8 mm and the mean annual observed runoff of 10.85 billion m^3 . The rainfall from April to June accounts for 50% of annual amount. The maximum observed runoff is $12\,100 \text{ m}^3 \text{ s}^{-1}$ and the maximum five-day observed runoff is 2.62 billion m^3 . Most heavy rainstorm emerges from May to July. In this area, the mean annual temperature is 16–20 17°C , with the maximum temperature of about 29°C emerging in July. The minimum mean monthly temperature of about $6\text{--}7^{\circ}\text{C}$ centers in January. The mean annual humidity is 80%, dispersing in the whole area evenly. The mean annual wind velocity is at Grade 2.1; in terms of the spatial distribution, the value is lower in the upper reaches and higher in the lower reaches.

A new approach to accurate validation

C. Sun et al.

[Title Page](#)

[Abstract](#)

[Introduction](#)

[Conclusions](#)

[References](#)

[Tables](#)

[Figures](#)

◀

▶

◀

▶

[Back](#)

[Close](#)

[Full Screen / Esc](#)

[Printer-friendly Version](#)

[Interactive Discussion](#)



2.2 Data acquisition

2.2.1 RS data

In the study, GMS-5 data were adopted as the data source for the ET retrieval. GMS data can be easily acquired with relatively high spatial resolution. In addition, the GMS data have accurate coordinates. The GMS-5 provides data in two grades of resolution: (1) the visible light band (VIS) with the spatial resolution of 1.25 km, the temporal resolution of 1 h, and the spectrum range from 0.55 μm to 1.05 μm ; (2) the thermal infrared band (TIR) with the spatial resolution of 5 km, the temporal resolution of 1h and the spectrum range from 10.5 μm to 12.5 μm ; (3) the water vapor band (WV) with the spatial resolution of 5 km, the temporal resolution of 1 h and the spectrum range from 6.2 μm to 7.6 μm . The visible light band was employed for the ET retrieval (Granger, 2000), and the water vapor band was employed for calibration and validation, as shown in Table 1.

2.2.2 Meteorologic data

The meteorologic data including daily precipitation, ET (obtained from retrieval), daily maximum temperature, daily minimum temperature, daily relative humidity, daily solar radiation and daily wind velocity, etc. were required in the study.

2.2.3 DEM data

DEM data were used in the process of evapotranspiration calculation and the SWAT-based hydrological simulation. The resolution of the DEM adopted in this study was 90 m, as shown in Fig. 2.

[Title Page](#)

[Abstract](#)

[Introduction](#)

[Conclusions](#)

[References](#)

[Tables](#)

[Figures](#)

[◀](#)

[▶](#)

[◀](#)

[▶](#)

[Back](#)

[Close](#)

[Full Screen / Esc](#)

[Printer-friendly Version](#)

[Interactive Discussion](#)



2.2.4 Landuse data

In the study, the landuse data, in accordance with the land classification specifications by the Chinese Academy of Sciences, included six landuse types: ploughland, woodland, grassland, water bodies, urban land and unused land. The scale of the landuse map was 1:100 000 in 2000. And for the SWAT model, the attribute codes of the landuse data should be converted to the US version, as shown in Fig. 2.

3 Model description and its analysis method

3.1 Data analysis and fusion model

The data validation analysis in this study includes two parts: the comparison between the ET results from RS retrieval and that obtained with the PM method, the comparison between simulated runoff and the observed runoff, as well as the comparison between the observed runoff and the runoff based on the PM-calculated ET using the data fusion method. The analysis flow and the new pattern are shown in Fig. 3. Three indications, including the Root Mean Square Error (RMSE), the mean deviation error (MBE) and R^2 , were employed for data analysis in this study.

3.2 RS retrieval model

A method based on the energy-balance theory developed by Wang and Jiang (2003, 2005) was adopted in this ET retrieval based on RS.

In this method, the RS-based latent heat flux was treated as the residual of the surface energy balance equation through model calculation (Kustas et al., 1994; Moran et al., 1994; Boegh et al., 2002). The surface energy of the earth is balanced through several different components, such as the net solar radiation flux and the energy consumption on the earth's surface, including the sensible heat flux, the latent heat flux, the

[Title Page](#)

[Abstract](#)

[Introduction](#)

[Conclusions](#)

[References](#)

[Tables](#)

[Figures](#)

[◀](#)

[▶](#)

[◀](#)

[▶](#)

[Back](#)

[Close](#)

[Full Screen / Esc](#)

[Printer-friendly Version](#)

[Interactive Discussion](#)



soil heat flux and the energy absorbed by vegetation. Accordingly, the energy balance equation can be expressed as:

$$LE = I_n - H - G - B \quad (1)$$

Where I_n is the net solar radiation flux, with W m^{-2} as the unit; H is the sensible heat flux, with W m^{-2} as the unit; LE is the latent heat flux, with W m^{-2} as the unit; G is the soil heat flux, with W m^{-2} as the unit; B is the energy absorbed by vegetation, with W m^{-2} as the unit.

According to the above energy-balance principle, the following steps are required to retrieve ET from RS data: first, the surface albedo (a), the vegetation index (NDVI) and the surface temperature (T_0) should be acquired through a specific RS channel; then, I_n , H , G and B as well as the instantaneous evapotranspiration (LE_x) are calculated, and the daily ET is calculated based on LE_x .

$$I_n = (1 - a)I_g - L_{\uparrow} + L_{\downarrow} \quad (2)$$

Where I_g is the total solar radiation, a is the albedo, L_{\uparrow} is the long-wave radiation of the earth surface, and L_{\downarrow} is the long-wave radiation of the atmosphere.

$$I_g = tS\cos(i_s) \quad (3)$$

where S is the solar constant (W m^{-2}), t is the transmission coefficient of the atmospheric radiation, and i_s is the solar altitude angle.

$$L_{\uparrow} = \varepsilon_0 \sigma T_0^4 \quad (4)$$

$$L_{\downarrow} = \varepsilon_0 \varepsilon_a \sigma T_a^4 \quad (5)$$

where T_0 is the surface temperature, T_a is the air temperature, ε_0 is the land surface emissivity, ε_a is the air emissivity, and σ is the Stefan-Boltzman constant.

The land surface temperature could be calculated according to the following formula:

$$L_{\uparrow}(T_0) = L_{\uparrow}(T_a) + (\partial L_{\uparrow} / \partial T)(T_0 - T_a) = (\varepsilon_0 \sigma T_a^4 + (4\varepsilon_0 \sigma T_{\text{avg}}^3))(T_0 - T_a) \quad (6)$$

A new approach to accurate validation

C. Sun et al.

[Title Page](#)

[Abstract](#)

[Introduction](#)

[Conclusions](#)

[References](#)

[Tables](#)

[Figures](#)

[◀](#)

[▶](#)

[◀](#)

[▶](#)

[Back](#)

[Close](#)

[Full Screen / Esc](#)

[Printer-friendly Version](#)

[Interactive Discussion](#)



The surface long-wave net radiation is given by:

$$L_n = (\varepsilon_0 \sigma T_a^4 + (4\varepsilon_0 \sigma T^3))(T_0 - T_a) - \varepsilon_0 \varepsilon_a \sigma T_a^4 = \varepsilon_0(1 - \varepsilon_a)\sigma T_a^4 + 4\varepsilon_0 \sigma T^3(T_0 - T_a) \quad (7)$$

where T_0 is the surface temperature; T_a is the air temperature; ε_0 is the surface emissivity; ε_a is the air emissivity and can be estimated with the Brunt formula, in which the air humidity adopts the observed climate data; σ is the Stefan-Boltzman constant.

According to the energy-balance principle, Brown and Rosenberg developed an impedance model for the sensible heat flux; Penmam-Monteith (Monteith, 1973) deduced a formula for H calculation:

$$H = -\rho C_p (T_a - T_0) / r_a \quad (8)$$

Where, T_0 is the ET surface temperature; T_a is the air temperature (at the attitude of 2.0 m); r_a is the surface roughness.

The heat flux $G_0(Z = 0)$ of the surface soil can be calculated according to the following formula:

$$G_0 = R_n \cdot [\Gamma_c + (1 - f_c) \cdot (\Gamma_s - \Gamma_c)] \quad (9)$$

Where, Γ_c is the canopy proportion coefficient; Γ_s is the bare-soil proportion coefficient; f_c is the vegetation coverage.

When the earth surface is covered by vegetation completely, $\Gamma_c = 0.05$ (Monteith, 1973); when the surface is bare soil, $\Gamma_s = 0.315$ (Kustas et al., 1999). In regions where the surface is partially covered by vegetation, f_c is obtained from RS data:

$$f_c = \frac{NDVI - NDVI_{min}}{NDVI_{max} - NDVI_{min}} \quad (10)$$

Where $NDVI_{max}$ and $NDVI_{min}$ are fixed at 0 and 0.5 according to the situations in China, respectively. For the RS data without near infrared bands, f_c could be deduced based on the landuse data in large scales (e.g., 1:100 000 or 1:10 000).

[Title Page](#)

[Abstract](#)

[Introduction](#)

[Conclusions](#)

[References](#)

[Tables](#)

[Figures](#)

[◀](#)

[▶](#)

[◀](#)

[▶](#)

[Back](#)

[Close](#)

[Full Screen / Esc](#)

[Printer-friendly Version](#)

[Interactive Discussion](#)



With the above parameters being settled, the daily evaporation (E_{daily} , mm/d) could be given by the following formula (Huang, 1997):

$$E_{\text{daily}} = 8.64 \times 10^7 \times \frac{24}{\Lambda} \times \frac{R_n - G_0}{\lambda \rho_w} \quad (11)$$

Where, $\frac{24}{\Lambda}$ is the daily evaporation ratio; R_n is the daily net radiation flux; G_0 is the daily soil heat flux; λ is the latent heat flux of vaporization (J Kg^{-1}); ρ_w is the water density (Kg m^{-3}).

3.3 PM model

The PM method is based on the presumption that all the energy for evaporation is accessible by the plant canopy, and that the water has to first diffuse through leaves against the surface resistance before diffusing into the atmosphere against the aerodynamic resistance (Shuttleworth, 1992). The PM equation is as follows:

$$ET_{\text{PM}} = \frac{\Delta A + \rho_a c_p (e_s - e_d) / r_a}{\lambda [\Delta + \gamma (1 + r_s / r_a)]} \quad (12)$$

where ET_{PM} is the daily ET (mm d^{-1}); ρ_a is the mean air density at constant pressure (kg m^{-3}); c_p is the specific heat of the air; r_s is the surface resistance (s m^{-1}); r_a is the aerodynamic resistance (s m^{-1}) and can be given by:

$$r_a = \frac{\ln[(z - d) / z_{0m}] \ln[(z - d) / z_{0v}]}{k^2 u} \quad (13)$$

Symbol z is the attitude for wind speed measurements (m); d is the zero-plane displacement height (m); z_{0m} is the roughness length for momentum transfer (m); z_{0v} is the roughness length for vapor transfer (m); k is the Van-Karman constant (0.41); u is

[Title Page](#)

[Abstract](#)

[Introduction](#)

[Conclusions](#)

[References](#)

[Tables](#)

[Figures](#)

[◀](#)

[▶](#)

[◀](#)

[▶](#)

[Back](#)

[Close](#)

[Full Screen / Esc](#)

[Printer-friendly Version](#)

[Interactive Discussion](#)



the wind speed (m s^{-1}). Based on the vegetation height (h , m), z_{0m} , z_{0v} and d can be estimated (Monteith, 1981; Plate, 1971):

$$\begin{cases} z_{0m} = 0.13h \\ z_{0v} = 0.1z_{0m} \\ d = 0.66h \end{cases} \quad (14)$$

Surface resistance r_s can be calculated as an inverse function of LAI (Jensen et al., 1990):

$$r_s = \frac{r_l}{0.5\text{LAI}} \quad (15)$$

where r_l is the minimum effective stomatal resistance of a single leaf (s m^{-1}), and LAI is the leaf area index of the canopy.

The PM method relies on a number of parameterizations taking into account environmental conditions. The values for the crop surface resistance, namely albedo and crop height, were set at 70 s m^{-1} , 0.23 and 0.12 m, resp., as recommended by Allen et al. (1998). As the primary energy source for ET, the shortwave radiation was estimated based on observed sunshine duration as well as an empirical relationship. Records of the temperature, relative humidity, air pressure, wind speed (measured at 10 m above the ground) and sunshine duration for each station were combined and reviewed for completeness and possible errors.

3.4 SWAT model

SWAT is a distributed hydrological model providing the spatial coverage of the integral hydrological cycle, including the atmosphere, plants, unsaturated zone, groundwater and surface water (Arnold et al., 1993; Neitsch et al., 2001a). The model is comprehensively described in literatures (Arnold et al., 1998; Neitsch et al., 2002) and widely used around the world, especially in humid areas (Heuvelmans, 2004; Van Liew, 2007;

A new approach to accurate validation

C. Sun et al.

[Title Page](#)

[Abstract](#)

[Introduction](#)

[Conclusions](#)

[References](#)

[Tables](#)

[Figures](#)

◀

▶

◀

▶

[Back](#)

[Close](#)

[Full Screen / Esc](#)

[Printer-friendly Version](#)

[Interactive Discussion](#)



Zhang, 2007). According to the water-balance principle, the principle of SWAT can be described as:

$$SW_t = SW_0 + \sum_{i=1}^t (R_{\text{day}} - Q_{\text{surf}} - E_a - w_{\text{seep}} - Q_{\text{gw}}) \quad (16)$$

Where, SW_t and SW_0 are the initial and the terminal water contents on day_i (mm); t is the time with a day as the unit; R_{day} is the rainfall on day_i (mm); Q_{surf} is the surface runoff on day_i (mm); E_a is the ET on day_i (mm); w_{seep} is the infiltration amount (mm); Q_{gw} is the runoff contribution from the groundwater (mm).

Under SWAT, conceptually, the catchment is subdivided into subbasins and a river network based on DEM. SWAT integrates the simulation of weather, crop growth, ET, surface runoff, percolation, return flow, erosion, nutrient transport, groundwater flow, pond and reservoir storage, channel routing, field drainage, the water consumption of plants and other supporting processes (Yuan, 1990). The tile drainage estimation is a function of the drain depth, the time needed for tile drains to bring the soil layer to field capacity and a drainage lag parameter. In SWAT, sub-catchments are divided into Hydrological Response Units (HRUs) as the unique combination of soil and land covers. The flow is not routed between HRUs, instead, the routing is used for flow in the channel network (Kannan et al., 2007b).

The input parameters of SWAT concern the ET studied in this paper, DEM, landuse data, soil data, property data, the observed data for the outlet of the basin, meteorological data such as daily precipitation, daily maximum and minimum temperature, wind velocity and relative humidity, as well as the runoff data on controlled sites and geographical materials, etc. The data required in SWAT for simulating the runoff and the data sources are shown Table 2.

The DEM of the catchment was prepared using the SRTM data with the spatial resolution of 90 m in the study area. Detailed landuse information, which was acquired from RESDC and CAS, was used to draw the landuse map and the soil map of the catchment. The Arc View-SWAT interface (AVSWAT-2000) was employed to delineate

[Title Page](#)

[Abstract](#)

[Introduction](#)

[Conclusions](#)

[References](#)

[Tables](#)

[Figures](#)

[◀](#)

[▶](#)

[◀](#)

[▶](#)

[Back](#)

[Close](#)

[Full Screen / Esc](#)

[Printer-friendly Version](#)

[Interactive Discussion](#)



the catchment boundaries, and the burning-in option was used to acquire the drainage network. A visual inspection of the derived drainage network and the network delineation on the paper map showed good agreement. The multiple HRU options available in the AV-SWAT interface were applied with the objective of representing each field as a separate HRU. As a result, the study area was discretized into 119 HRUs, as shown in Fig. 7.

4 Results

4.1 Results of two ET methods

The monthly ET results from 2000 to 2004 in the Zhelin Basin obtained with the two approaches, namely the RS retrieval method and the familiar Penman-Monteith ET model, were analyzed in the following Figs. 4 and 5. The whole Zhelin Basin involved 238 RS pixels, and the result of the RS retrieval of ET was the mean of the 238 pixels; the PM result was the output of the PM model.

The monthly ET from the RS retrieval in March, June, September and December of 2000 were selected to represent the four seasons, respectively, as shown in Fig. 4. 238 pixels in total were included in each map. The monthly ET results from the RS retrieval and the Penman-Monteith method from 2000 to 2004 were shown in Fig. 5.

The spatial distribution of the monthly ET was analyzed. In March, when the rainfall was relatively less throughout the whole year, the maximum ET emerged in the area with plenty of water, such as reservoirs and paddy fields, while the minimum ET appeared in the upper reaches of the basin and the area with high altitudes, as shown in Fig. 4a, which indicated that the primary factor affecting ET is the water capacity in this season. In June and September when the rainfall is abundant and the temperature is high throughout the year, the ET distribution was uniform in the basin, as shown in Fig. 4b and c. In December when the temperature was the lowest and the rainfall is the least among the year, as shown in Fig. 4d, the maximum ET emerged in the upper

A new approach to accurate validation

C. Sun et al.

[Title Page](#)

[Abstract](#)

[Introduction](#)

[Conclusions](#)

[References](#)

[Tables](#)

[Figures](#)

[◀](#)

[▶](#)

[◀](#)

[▶](#)

[Back](#)

[Close](#)

[Full Screen / Esc](#)

[Printer-friendly Version](#)

[Interactive Discussion](#)



reaches of the basin and the area with high altitudes, and the total ET was the least among the year due to the low temperature; in this period, the altitude was the major factor affecting the ET distribution in the whole basin.

The seasonal variation of ET was analyzed, as shown in Fig. 5. The ET exhibited an obvious rule of seasonal variation, i.e., the maximum ET emerged in Summer when the temperature is highest and the rainfall is abundant, the ET was less in Spring and Autumn than in Summer, and the ET reached the least throughout the year in Winter. In other words, the variation trend of the ET was coordinated with the rainfall and temperature variation in a year.

From the figures and data above, it could be inferred that the ET results calculated in PM method was lower compared with those from RS retrieval in the five years, which was consistent with the results of previous studies (Dugas and Ainsworth, 1985; Benson et al., 1992).

4.2 Result of runoff simulation with two ET methods based on SWAT and observed runoff

Due to the regional adaptability, the SWAT model should be calibrated and validated before using. In this study, the data from 2001 to 2004 were adopted for calibration, and the data of 2000 were adopted for validation. According to Nash and Sutcliffe (1970), the model would be evaluated with the following parameters: model efficiency coefficient Ens, mean error Re and correlation coefficient R^2 which was calculated using excel, while Re and Ens were calculated according to the following formula:

$$R_e = \frac{Q_{\text{sim},i} - Q_{\text{obs},i}}{Q_{\text{obs},i}} \times 100\% \quad \text{Ens} = 1 - \frac{\sum_{i=1}^n (Q_{\text{obs},i} - Q_{\text{sim},i})^2}{\sum_{i=1}^n (Q_{\text{obs},i} - \bar{Q}_{\text{obs}})^2} \quad (17)$$

[Title Page](#)

[Abstract](#)

[Introduction](#)

[Conclusions](#)

[References](#)

[Tables](#)

[Figures](#)

[◀](#)

[▶](#)

[◀](#)

[▶](#)

[Back](#)

[Close](#)

[Full Screen / Esc](#)

[Printer-friendly Version](#)

[Interactive Discussion](#)



where, $Q_{\text{obs},i}$ is the observed runoff, $Q_{\text{sim},i}$ is the simulated runoff, and \bar{Q}_{obs} is the average observed runoff.

In SWAT, the whole basin was divided into 119 HRUs, as shown in Fig. 6. The accepted range after calibration was shown in Table 3.

5 After the calibration and validation, the evaluation indicators of SWAT were shown in Table 4, with good general performance.

On the basis above, the data of the monthly simulated runoff using SWAT and the observed data in the Zhelin Basin from 2000 to 2004 were shown in Fig. 7.

5 Discussions

10 5.1 Comparison of ET from RS retrieval and from calculation of PM model

The monthly results obtained with the PM-based ET model and those obtained with the RS retrieval method were compared as follows.

15 The monthly ET results retrieved from the data of 238 RS pixels versus the results calculated with the PM model were analyzed, as shown in the following Fig. 8. Table 5 showed the value of RMSE, MBE and R^2 from the comparison of the monthly ET data calculated with the Penman-Monteith method and RS retrieval, for the Zhelin Basin from 2000 to 2004.

20 The monthly ET results obtained from the PM model and those with the RS retrieval were compared, as shown in Fig. 8, and key parameters were shown in Table 5. The RMSE, MBE and R^2 for the results obtained with the two methods were 17.30975, 14.53333 and 0.8194, respectively, as shown in Figs. 5, 8 and Table 5. The correlation coefficient between the two results was satisfactory, with R^2 amounting to 0.8194. These results suggested that the monthly ET from the RS retrieval had good correlation with that from the PM method, which could be explained by the less influence of 25 clouds and the persistent influence by limited meteorologic stations from a long time

A new approach to accurate validation

C. Sun et al.

[Title Page](#)

[Abstract](#)

[Introduction](#)

[Conclusions](#)

[References](#)

[Tables](#)

[Figures](#)

◀

▶

◀

▶

[Back](#)

[Close](#)

[Full Screen / Esc](#)

[Printer-friendly Version](#)

[Interactive Discussion](#)



scale. Besides, the RS retrieval results were still higher than the PM-based results, which was coordinated with previous studies (Jamieson, 1982; Dugas and Ainsworth, 1985; Benson et al., 1992; Pereira and Nova, 1992).

5.2 Comparison of simulated runoff with observed data after data fusion

5 According to the analysis in Sect. 5.1, the correlation between the monthly ET data obtained with the two methods was satisfactory. Therefore, in order to embody the representativeness of the study and improve the reliability, the monthly data were adopted in the runoff simulation. The monthly runoff data and the simulated runoff data with SWAT using the two ET methods in the Zhelin Basin from 2000 to 2004 were shown in
10 comparison in Fig. 9.

From the figure and table above, the correlation ($R^2=0.8516$) between the simulated results based on ET retrieval and the observed data was higher than the that ($R^2=0.8411$) between the results simulated with PM-based ET and the observed data after data fusion. The RMSE (RMSE=26.0860) between the simulated runoff based on ET retrieval and the observed data was obviously smaller than the that (RMSE=35.71904) between the runoff simulated with PM-based ET and the observed data. The MBE (MBE=−8.6578) between the simulated runoff based on ET retrieval and the observed data was obviously superior to that (MBE=−22.7313) between the simulated runoff based PM-based ET and the observed data, as shown in Fig. 9 and
15 Table 6.

Currently, there is no way to validate the retrieval results pixel by pixel directly. However, the underlying conditions of the basin can be taken into account in the distributed hydrological model with high sensitivity to the accuracy of the input data, so that the retrieval results can be validated indirectly through data fusion and with the support of
20 the distributed hydrological model. According to the runoff analysis based on SWAT, the RS retrieval method had advantages in calculating the ET in this area compared with the PM-based method, i.e., the ET results obtained with this method exhibited better adaptivity and accuracy than the PM-based one, which might attribute to the
25

[Title Page](#)

[Abstract](#)

[Introduction](#)

[Conclusions](#)

[References](#)

[Tables](#)

[Figures](#)

[◀](#)

[▶](#)

[◀](#)

[▶](#)

[Back](#)

[Close](#)

[Full Screen / Esc](#)

[Printer-friendly Version](#)

[Interactive Discussion](#)



high resolution of the 238 RS pixels, while in contrast, the data obtained with PM were based only on one meteorologic station in the study area.

The PM method was a widely recognized model for ET calculation. However, the results of this study showed that the RS retrieval method performed better than the PM method in the study area. Therefore, it could be deduced that the RS retrieval was an adaptive and highly accurate ET retrieving method. In addition, SWAT is also a widely applied hydrological model instead of being exclusively designed for this RS retrieval of ET. It is possible that, if other more suitable hydrological models were adopted or a hydrological model exclusively for RS retrieval of ET was designed, the simulation results would be even better.

According to the analysis above, the RS retrieval method was a good approach to ET calculation because of its high spatial resolution, with the RMSE, MBE and R^2 of runoff all being superior to the PM model. On the other hand, the SWAT model was excellent in fusing several sorts of data, especially the ET data to validate the ET results obtained from RS retrieval. In conclusion, it was a good pattern to validate the results of ET retrieval based on data fusion.

6 Conclusions

This study presented a new method using data fusion to validate the ET results from RS retrieval with the support of a distributed hydrological model SWAT.

First, ET data in five years (2000–2004) were acquired with the RS retrieval according to the principle of energy balance. The temporal/spatial distribution of the monthly ET and corresponding dominant influencing factors were analyzed in the year of 2000, and five years of monthly ET was also calculated with the PM model. Subsequently, the ET from RS retrieval and the PM-based ET were compared. Finally, the ET obtained with RS retrieval was accurately validated with the new method, under the support of SWAT.

[Title Page](#)

[Abstract](#)

[Introduction](#)

[Conclusions](#)

[References](#)

[Tables](#)

[Figures](#)

[◀](#)

[▶](#)

[◀](#)

[▶](#)

[Back](#)

[Close](#)

[Full Screen / Esc](#)

[Printer-friendly Version](#)

[Interactive Discussion](#)



According to the ET data analysis, it could be seen that the correlation R^2 between the monthly ET data acquired with the two methods was high, with R^2 amounting to 0.8914, which could be explained by the less influence from the clouds and the persistent influence of inadequate representativeness of meteorologic stations. Moreover, 5 the PM-based ET was smaller than the result from ET retrieval, which was coordinated with previous studies (Jamieson, 1982; Dugas and Ainsworth, 1985; Benson et al., 1992; Pereira and Nova, 1992).

After data fusion, it could be deduced through comparison that the RS method had better adaptability and accuracy than the PM-based method, which might due to the 10 high resolution of 238 RS pixels, while the data from PM method were based only on one meteorologic station in the study area.

In conclusion, the RS retrieval method adopted in this paper was a good method in calculating ET. Owing to the high resolution of the RS data, the runoff data obtained from RS retrieval of ET after data fusion was better than those from PM-based ET in 15 terms of the parameters: RMSE, MBE and R^2 . Besides, SWAT was a model suitable for data fusion. The new pattern of validating ET retrieval results using the distributed hydrological model based on data fusion was feasible and reliable, which deserves further studies.

The subsequent research work of this study should be focused on improving the 20 temporal/spatial resolution of the remote sensing data, i.e., improving the accuracy or reliability of the retrieval result, and enhance the improvement of ET retrieval from remote sensing data

Acknowledgements. This paper was funded by the Earth System Science Data Sharing Program of China (2005DKA32300, <http://www.geodata.cn>); the National Natural Science Foundation Program of China (40801180, 40771146). 25

[Title Page](#)

[Abstract](#)

[Introduction](#)

[Conclusions](#)

[References](#)

[Tables](#)

[Figures](#)

[◀](#)

[▶](#)

[◀](#)

[▶](#)

[Back](#)

[Close](#)

[Full Screen / Esc](#)

[Printer-friendly Version](#)

[Interactive Discussion](#)



Allen, R. G., Pereira, L. S., Raes, D., and Smith, M.: Crop evapotranspiration: Guidelines for computing crop water requirements, FAO Irrigation and Drainage Paper no. 56, Rome, 1998.

Allen, R. G., Tasumi, M., Morse, A., and Trezza, R.: A landsat-based energy balance and evapotranspiration model in Western US water rights regulation and planning, *Irrig. Drain. Syst.*, 19(3–4): 251–268, 2005..

Amatya, D. M., Skaggs, R. W., and Gregory, J. D.: Comparison of methods for estimating REF-ET., *J. Irrig. Drain. E.-ASCE*, 121(6), 427–435, 1995.

Arnold, J. G., Allen, P. M., and Bernhardt, G.: A comprehensive surface-groundwater flow model, *J. Hydrol.*, 142, 47–69, 1993.

Arnold, J. G., Srinivasan, R., Muttiah, R. S., and Williams J. R.: Large area hydrologic modeling and assessment part I: model development, *J. Am. Water Resour. As.*, 34(1), 73–89, 1998.

Bastiaanssen, W. G. M., Menenti, M., Feddes, R. A., and Holtslag, A. A.: A remote sensing surface energy balance algorithm for land (SEBAL), *J. Hydrol.*, 212–213, 198–212, 1998a.

Bastiaanssen, W. G. M., Pelgrum, H., Wang, J., Ma, Y., Moreno, J. F., Roerink, G. J., and van der Wal, T.: A remote sensing surface energy balance algorithm for land (SEBAL), IIValidation, *J. Hydrol.*, 212–213, 213–229, 1998b.

Bastiaanssen, W. G. M.: SEBAL-based sensible and latent heat fluxes in the irrigated Gediz Basin, Turkey, *J. Hydrol.*, 2229, 87–100, 2000.

Batra, N., Islam, S., Venturini, V., Bisht, G., and Jiang, L.: Estimation and comparison of evapotranspiration from MODIS and AVHRR sensors for clear sky days over the Southern Great Plains, *Remote Sens. Environ.*, 103, 1–15, 2006.

Benson, V. W., Potter, K. N., Bogusch, H. C., Goss, D., and Williams, J. R.: Nitrogen leaching sensitivity to evapotranspiration and soil water storage estimates in EPIC, *J. Soil Water Conserv.*, 47, 334–337, 1992.

Boegh, E., Poulsen, R. N., Butts, M., et al.: Remote sensing based evapotranspiration and runoff modeling of agricultural, forest and urban flux sites in Denmark: From field to macro-scale, *J. Hydrol.*, 377, 300–316, 2009.

Boegh, E., Soegaard, H., and Thomsen, A.: Evaluating evapotranspiration rates and surface condition suing Landsat TM to estimate atmospheric resistance and surface resistance, *Remote Sens. Environ.*, 70, 329–343, 2002.

A new approach to accurate validation

C. Sun et al.

[Title Page](#)[Abstract](#)[Introduction](#)[Conclusions](#)[References](#)[Tables](#)[Figures](#)[◀](#)[▶](#)[◀](#)[▶](#)[Back](#)[Close](#)[Full Screen / Esc](#)[Printer-friendly Version](#)[Interactive Discussion](#)

DehghaniSanij, H., Yamamoto, T., and Rasiah, V.: Assessment of evapotranspiration estimation models for use in semiarid environments, *Agr. Water Manage.*, 64, 91–106, 2004.

5 Drexler, J. Z., Snyder, R. L., Spano, D., and Paw, K. T. U.: A review of models and micrometeorological methods used to estimate wetland evapotranspiration, *Hydrol. Process.*, 18(11), 2071–2101, 2004.

Dugas, W. A. and Ainsworth, C. G.: Effect of potential evapotranspiration estimates on crop simulation models, *Trans. ASAE*, 28, 471–475, 1985.

10 Fichlin, D. L., Luo, Y. Z., Luedeling, E., et al.: Climate change sensitivity assessment of a highly agricultural watershed using SWAT, *J. Hydrol.*, 374, 16–29, 2009.

Gao, Y. C. and Long, D.: Intercomparison of remote sensing-based models for estimation of evapotranspiration and accuracy assessment based on SWAT, *Hydrol. Process.*, 22, 4850–4869, 2008.

15 Garatuza-Payan, J., Shuttleworth, W. J., Encinas, D., McNeil, D. D., Stewart, J. B., deBruin, H., and Watts, C.: Measurement and modelling evaporation for irrigated crops in north-west Mexico, *Hydrol. Process.*, 12(9), 1397–1418, 1998.

Garcia, M., Raes, D., Allen, R., and Herbas, C.: Dynamics of reference evapotranspiration in the Bolivian highlands (Altiplano), *Agr. Forest Meteorol.*, 125, 67–82, 2004.

20 Garatuza-Payan, J. and Watts, C. J.: The use of remote sensing for estimating ET of irrigated wheat and cotton in Northwest Mexico, *Irrig. Drain. Syst.*, 19(3–4), 301–320, 2005.

Gavila'n, P., Lorite, I. J., Tornero, S., et al.: Regional calibration of Hargreaves equation for estimating reference ET in a semiarid environment, *Agr. Water Manage.*, 81, 257–281, 2006.

Guan, H. D. and Wilson, J. L.: A hybrid dual-source model for potential evaporation and transpiration partitioning, *J. Hydrol.*, 377, 405–416, 2009.

25 Granger, R. J.: A feedback approach for the estimate of evapotranspiration using remotely-sensed data, in: Application of remote sensing in hydrology, edited by: Kite, G. W., Pietroniro, A., and Pultz, T. J., Proceedings of the Second International Workshop, NHRI Symposium No. 14, Saskatoon, 18–19 October 1994, NHRI, 211–222, 1995.

A new approach to accurate validation

C. Sun et al.

[Title Page](#)

[Abstract](#)

[Introduction](#)

[Conclusions](#)

[References](#)

[Tables](#)

[Figures](#)

[◀](#)

[▶](#)

[◀](#)

[▶](#)

[Back](#)

[Close](#)

[Full Screen / Esc](#)

[Printer-friendly Version](#)

[Interactive Discussion](#)



Granger, R. J.: Comparison of surface and satellite-derived estimates of evapotranspiration using a feedback algorithm, in: Application of remote sensing in hydrology, edited by: Kite, G. W., Pietroniro, A., and Pultz, T. J., Proceedings of the Third International Workshop, NHRI Symposium No. 17, October 1996; NASA, Goddard Space Flight Center, Greenbelt, MD, NHRI, 71–81, 1997.

5 Granger, R. J.: Satellite-derived estimates of evapotranspiration in the Gediz basin, *J. Hydrol.*, 229, 70–76, 2000.

George, B. A., Reddy, B. R. S., Raghuvanshi, N. S., and Wallender, W. W.: Decision support system for estimating reference evapotranspiration, *J. Irrig. Drain. E.-ASCE*, 128(1), 1–10, 10 2002.

Hargreaves, G. L. and Samani, Z. A.: Estimating potential evapotranspiration, *J. Irrig. Drain. E.-ASCE*, 108(3), 225–230, 1982.

Heilman, J. L., McInnes, K. J., Kjelgaard, J. F., et al.: Energy balance and water use in a subtropical karst woodland on the Edwards Plateau, Texas, *J. Hydrol.*, 373, 426–435, 2009.

15 Heuvelmans, G., Muys, B., and Feyen, J.: Analysis of the spatial variation in the parameters of the SWAT model with application in Flanders, Northern Belgium, *Hydrol. Earth Syst. Sci.*, 8, 931–939, 2004,
<http://www.hydrol-earth-syst-sci.net/8/931/2004/>.

Huang, H. F.: Principle and model on the interaction among the Soil-Vegetation-Atmosphere, 20 the Meteorologic Press, Beijing, 1997 (in Chinese).

Hussey, B. H. and Odum, W. E.: Evapotranspiration in Tidal Marshes, *Estuaries*, 15(1), 59–67, 1992.

Immerzeel, W. W. and Droogers, P.: Calibration of a distributed hydrological model based on satellite evapotranspiration, *J. Hydrol.*, 349, 411–424, 2008.

25 Jabloun, M. and Sahli, A.: Evaluation of FAO-56 methodology for estimating reference evapotranspiration using limited climatic data Application to Tunisia, *Agr. Water Manage.*, 95, 707–715, 2008.

Jacob, F., Olioso, A., Gu, X. F., Su, Z. B., and Seguin, B.: Mapping surface fluxes using airborne 30 visible, near infrared, thermal infrared remote sensing data and a spatialized surface energy balance model, *Agronomie*, 22(6), 669–680, 2002b.

Jamieson, P. D.: Comparison of methods of estimating maximum evaporation from a barley crop, *NZ J. Sci.*, 25, 175–181, 1982.

A new approach to accurate validation

C. Sun et al.

[Title Page](#)

[Abstract](#)

[Introduction](#)

[Conclusions](#)

[References](#)

[Tables](#)

[Figures](#)

◀

▶

◀

▶

[Back](#)

[Close](#)

[Full Screen / Esc](#)

[Printer-friendly Version](#)

[Interactive Discussion](#)



Jensen, M. E., Burman, R. D., and Allen, R. G. (Eds.): Evapotranspiration and irrigation water requirements. ASCE Manuals and Reports on Engineering Practice No. 70, ASCE, New York, 332 pp., 1990.

5 Jiang, D., Wang, J. H., Yang X. H., et al.: Key hydrological parameters retrieved by using remote sensing technique in the Yellow River Basin, *Advances in water Science*, 14(6), 736–739, 2003 (in Chinese, Abstract in English).

10 Kannan, N., White, S. M., Worrall, F., et al.: Sensitivity analysis and identification of the best evapotranspiration and runoff options for hydrological modeling in SWAT-2000, *J. Hydrol.*, 332, 456–466, 2007a.

15 Kannan, N., White, S. M., Worrall, F., et al.: Hydrological modeling of a small catchment using SWAT-2000 – Ensuring correct flow partitioning for contaminant modeling, *J. Hydrol.*, 334, 64–72, 2007b.

20 Kite, G. W. and Droogers, P.: Comparing evapotranspiration estimates from satellites, hydrological models and field data, *J. Hydrol.*, 229, 3–18, 2000.

25 Kustas, W. P., Moran, M. S., Humes, K. S., Stannard, D. I., Pinter Jr., P. J., Hipps, L. E., Swiatek, E., and Goodrich, D. C.: Surface energy balance estimates at local and regional scales using optical remote sensing from an aircraft platform and atmospheric data collected over semiarid rangelands, *Water. Resour. Res.*, 30(5), 1241–1259, 1994.

30 Kustas, W. P. and Norman, J. M.: Evaluation of soil and vegetation heat flux predictions using a simple two-source model with radiometric temperatures for partial canopy cover, *J. Agr. Forest Meteorol.*, 94, 13–29, 1999.

Liu, R., Wen, J., Wang, X., Wang, L., Tian, H., Zhang, T. T., Shi, X. K., Zhang, J. H., and Lv, SH. N.: Actual daily evapotranspiration estimated from MERIS and AATSR data over the Chinese Loess Plateau, *Hydrol. Earth Syst. Sci.*, 14, 47–58, 2010, <http://www.hydrol-earth-syst-sci.net/14/47/2010/>.

Mohan, S.: Intercomparison of evapotranspiration estimates, *Hydrolog. Sci. J.*, 36(5), 447–460, 1991.

Monteith, J. L.: *Principles of Environmental Physics*, Edward Arnold, London, 1973.

Monteith, J. L.: Evaporation and surface temperature, *Q. J. Roy. Meteor. Soc.*, 107, 1–27, 1981.

Moran, M. S., Kustas, W. P., Vidal, A., Stannard, D. I., Blanford, J. H., and Nichols, W. D.: Use of ground-based remotely sensed data for surface energy balance evaluation of a semiarid rangeland, *Water. Resour. Res.*, 30(5), 1339–1349, 1994.

A new approach to accurate validation

C. Sun et al.

[Title Page](#)

[Abstract](#)

[Introduction](#)

[Conclusions](#)

[References](#)

[Tables](#)

[Figures](#)

[◀](#)

[▶](#)

[◀](#)

[▶](#)

[Back](#)

[Close](#)

[Full Screen / Esc](#)

[Printer-friendly Version](#)

[Interactive Discussion](#)



Nash, J. E. and Sutcliffe, J. V.: River flow forecasting through conceptual models, *J. Hydrol.*, 10(3), 282–290, 1970.

Neale, C., Jayanthi, H., and Wright, J. L.: Irrigation water management using high resolution airborne remote sensing, *Irrig. Drain. Syst.*, 19(3–4), 321–336, 2005.

5 Neitsch, S. L., Arnold, J. G., Kiniry, J. R., et al.: Soil and Water Assessment Tool-Version 2000-User's Manual, Temple, TX, USA, 2001a.

Neitsch, S. L., Arnold, J. G., Kiniry, J. R., et al.: Soil and water assessment tool, Theoretical documentation, Version 2000, 2002.

10 Overgaard, J., Rosbjerg, D., and Butts, M. B.: Land-surface modelling in hydrological perspective – a review, *Biogeosciences*, 3, 229–241, 2006,
<http://www.biogeosciences.net/3/229/2006/>.

Parasuraman, K., Elshorbagy, A., and Carey, S. K.: Modelling the dynamics of the evapotranspiration process using genetic programming, *Hydrolog. Sci. J.*, 52(3), 563–578, 2007.

Pereira, A. R. and Nova, N. A. V.: Analysis of the Priestley-Taylor parameter, *Agr. Forest Meteorol.*, 61, 1–9, 1992.

15 Plate, E. J.: Aerodynamic characteristics of atmospheric boundary layers, US Atomic Energy Comm., Critical Revies Series, TID-25465, US Department of Energy, Springfield, 190 pp., 1971.

Shuttleworth, W. J., Evaporation, in: *Handbook of Hydrology*, edited by: Maidment, D. R.,
20 McGraw-Hill, New York, NY, 4.1–4.53, 1992.

Su, Z.: The Surface Energy Balance System (SEBS) for estimation of turbulent heat fluxes, *Hydrol. Earth Syst. Sci.*, 6, 85–100, 2002,
<http://www.hydrol-earth-syst-sci.net/6/85/2002/>.

25 Sun, L. and Song, C. C.: Evapotranspiration from a freshwater marsh in the Sanjiang Plain, Northeast China, *J. Hydrol.*, 352, 202–210, 2008.

Teresa, A. P., Teresa, S. D., Manuel O. H., et al.: Evapotranspiration from a Mediterranean evergreen oak savannah :The role of trees and pasture, *J. Hydrol.*, 369, 98–106, 2009.

Van Liew, M. W., Veith, T. L., Bosch, D. D., et al.: Suitability of SWAT for the conservation effects assessment project: comparison on USDA agricultural research service watersheds, *J. Hydrol. Eng.*, 12(2), 173–189, 2007.

30 Wang, J. H. Jiang, D.: Study on the duality water circulation of the Yellow river basin, The Science Press, Beijing, 2005 (in Chinese).

A new approach to accurate validation

C. Sun et al.

[Title Page](#)[Abstract](#)[Introduction](#)[Conclusions](#)[References](#)[Tables](#)[Figures](#)[◀](#)[▶](#)[◀](#)[▶](#)[Back](#)[Close](#)[Full Screen / Esc](#)[Printer-friendly Version](#)[Interactive Discussion](#)

Wei, W., Charles, A. S. H., Frederick, N. S., et al.: Spatial modelling of evapotranspiration in the Luquillo experimental forest of Puerto Rico using remotely-sensed data, *J. Hydrol.*, 328, 733–752, 2006.

5 Yagob, D.: Study of reference crop evapotranspiration in I.R. of Iran, *Agr. Water Manage.*, 84, 123–129, 2006.

Yuan, Z. X.: *Basin Hydrologic Model*, China WaterPower Press, Beijing, 1990 (in Chinese).

Zhang, M. X.: Runoff Simulation based on SWAT model in the Xixi Watershed of the Jinjiang River, Fujian Normal University, 2007 (in Chinese, Abstract in English).

10 Zhou, L. and Zhou, G. S.: Measurement and modeling of evapotranspiration over a reed(*Phragmites australis*) marsh in Northeast China, *J. Hydrol.*, 372, 41–47, 2009.

A new approach to accurate validation

C. Sun et al.

[Title Page](#)[Abstract](#)[Introduction](#)[Conclusions](#)[References](#)[Tables](#)[Figures](#)[|◀](#)[▶|](#)[◀](#)[▶](#)[Back](#)[Close](#)[Full Screen / Esc](#)[Printer-friendly Version](#)[Interactive Discussion](#)

A new approach to accurate validation

C. Sun et al.

Table 1. The spatial resolution and purpose of the three spectrum on GMS image.

Band's name	Visible band	Thermal infrared band	Vapour band
Spatial resolution (km)	1.25	5	5
Purpose	Evapotranspiration retrieval	Evapotranspiration retrieval	Validation

[Title Page](#)[Abstract](#)[Introduction](#)[Conclusions](#)[References](#)[Tables](#)[Figures](#)[|◀](#)[▶|](#)[◀](#)[▶](#)[Back](#)[Close](#)[Full Screen / Esc](#)[Printer-friendly Version](#)[Interactive Discussion](#)

A new approach to accurate validation

C. Sun et al.

Table 2. The SWAT needed data and their source information.

Data type	DEM	Landuse data	Property data	Soil data
Sources	http://www.geodata.cn	http://www.geodata.cn & RESDC,CAS	http://www.geodata.cn & RESDC,CAS	http://www.geodata.cn
Data type	Observed data	Meteorological data	Runoff data	ET
Sources	the information center of the Institute of Water Resources and Hydropower Research and the information center of Zhelin HydroPower Corp	The China meteorological administration; the information center of the Institute of Water Resources and Hydropower Research and the information center of Zhelin HydroPower Corp; the information center of the Institute of Water Resources and Hydropower Research and the information center of Zhelin HydroPower Corp;	the information center of the Institute of Water Resources and Hydropower Research and the information center of Zhelin HydroPower Corp	Retrieved in this study.

[Title Page](#)[Abstract](#)[Introduction](#)[Conclusions](#)[References](#)[Tables](#)[Figures](#)[|◀](#)[▶|](#)[◀](#)[▶](#)[Back](#)[Close](#)[Full Screen / Esc](#)[Printer-friendly Version](#)[Interactive Discussion](#)

A new approach to accurate validation

C. Sun et al.

Table 3. Calibrated parameters of the model.

Parameter	Value scope	Value
ESCO	0~1	0.1
SCS Runoff Curve: CN ₂	-8~8	-7
Baseflow a Coffecient: ALPHA BF	0~1	0.041
Soil Available Water Capacity: SOL_AWC	0~1	0.04

[Title Page](#)[Abstract](#)[Introduction](#)[Conclusions](#)[References](#)[Tables](#)[Figures](#)[|◀](#)[▶|](#)[◀](#)[▶](#)[Back](#)[Close](#)[Full Screen / Esc](#)[Printer-friendly Version](#)[Interactive Discussion](#)

A new approach to accurate validation

C. Sun et al.

Table 4. Estimation of the model simulated result.

Period of time	Re	Ens	R^2
Calibration	0.119	0.875	0.946
Validation	0.101	0.808	0.925

[Title Page](#)[Abstract](#)[Introduction](#)[Conclusions](#)[References](#)[Tables](#)[Figures](#)[|◀](#)[▶|](#)[◀](#)[▶](#)[Back](#)[Close](#)[Full Screen / Esc](#)[Printer-friendly Version](#)[Interactive Discussion](#)

A new approach to accurate validation

C. Sun et al.

Table 5. Table of the RMSE, MBE, R^2 among the monthly ET data calculated with Penman-monteith, versus the ET data based on remote sensing data method from 2000 to 2004 in Zhelin basin.

Time Type	RMSE	MBE	R^2
Monthly	17.30975	14.53333	0.8194

[Title Page](#)[Abstract](#)[Introduction](#)[Conclusions](#)[References](#)[Tables](#)[Figures](#)[|◀](#)[▶|](#)[◀](#)[▶](#)[Back](#)[Close](#)[Full Screen / Esc](#)[Printer-friendly Version](#)[Interactive Discussion](#)

A new approach to accurate validation

C. Sun et al.

Table 6. Table of the RMSE, MBE, R^2 among the runoff data simulated with Penman-monteith ET, and remote sensing based ET respectively on SWAT versus the observed data from 2000 to 2004 in Zhelin basin.

Model Type	RMSE	MBE	R^2
Penman-monteith	35.71904	-22.7313	0.8411
Remote sensing based	26.0860	-8.6578	0.8516

[Title Page](#)[Abstract](#)[Introduction](#)[Conclusions](#)[References](#)[Tables](#)[Figures](#)[|◀](#)[▶|](#)[◀](#)[▶](#)[Back](#)[Close](#)[Full Screen / Esc](#)[Printer-friendly Version](#)[Interactive Discussion](#)

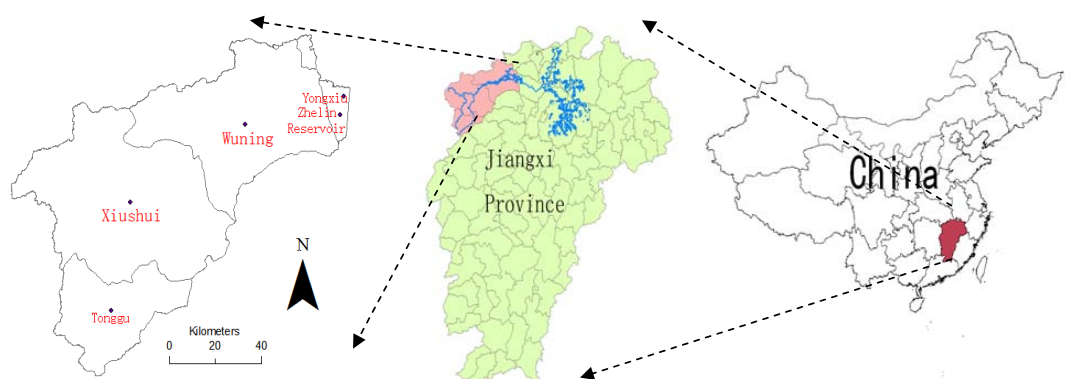


Fig. 1. The sketch map of Zhelin basin and its location.

A new approach to accurate validation

C. Sun et al.

[Title Page](#)

[Abstract](#)

[Introduction](#)

[Conclusions](#)

[References](#)

[Tables](#)

[Figures](#)

[◀](#)

[▶](#)

[◀](#)

[▶](#)

[Back](#)

[Close](#)

[Full Screen / Esc](#)

[Printer-friendly Version](#)

[Interactive Discussion](#)



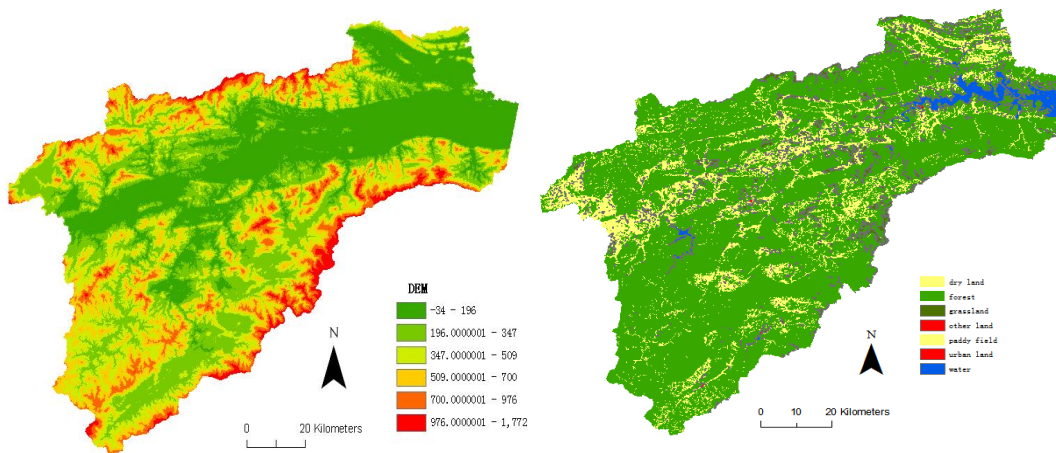


Fig. 2. The DEM and Landuse of Zhelin basin.

A new approach to accurate validation

C. Sun et al.

[Title Page](#)

[Abstract](#)

[Introduction](#)

[Conclusions](#)

[References](#)

[Tables](#)

[Figures](#)

◀

▶

◀

▶

[Back](#)

[Close](#)

[Full Screen / Esc](#)

[Printer-friendly Version](#)

[Interactive Discussion](#)



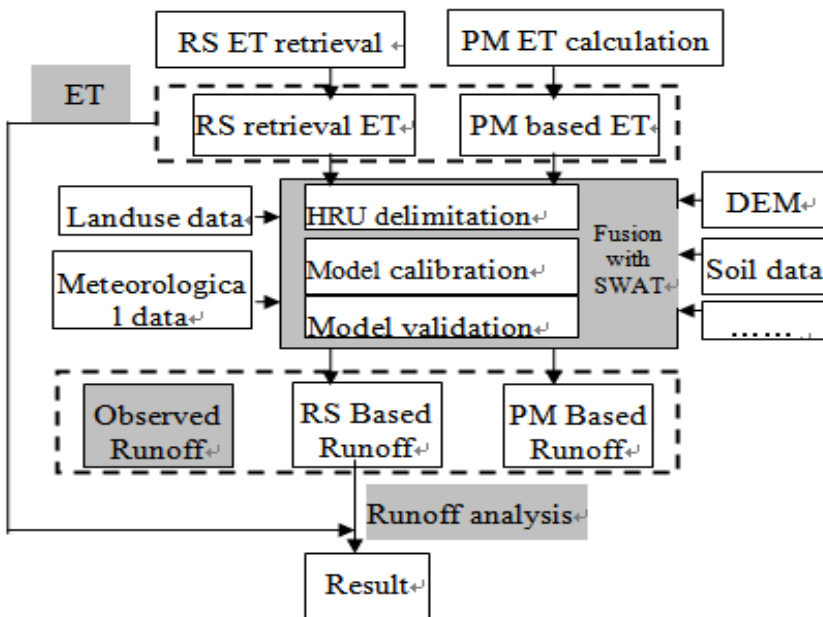


Fig. 3. The analysis method and data fusion.

A new approach to accurate validation

C. Sun et al.

[Title Page](#)

[Abstract](#)

[Introduction](#)

[Conclusions](#)

[References](#)

[Tables](#)

[Figures](#)

[|◀](#)

[▶|](#)

[◀](#)

[▶](#)

[Back](#)

[Close](#)

[Full Screen / Esc](#)

[Printer-friendly Version](#)

[Interactive Discussion](#)



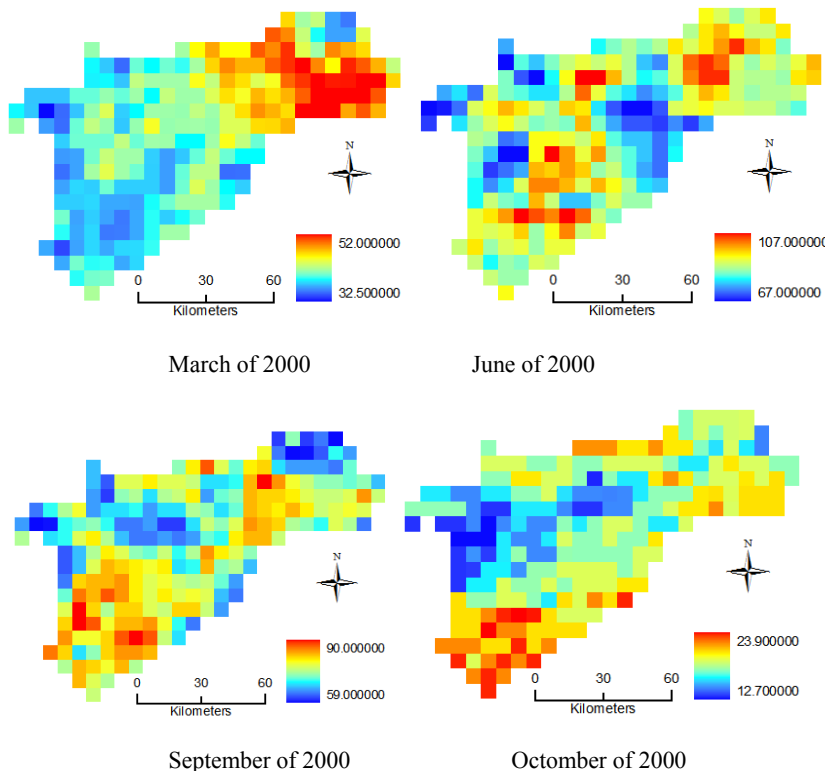


Fig. 4. The selected monthly ET result from the remote sensing based method on March, June, September, and December of the year 2000.

A new approach to accurate validation

C. Sun et al.

[Title Page](#)

[Abstract](#)

[Introduction](#)

[Conclusions](#)

[References](#)

[Tables](#)

[Figures](#)

[◀](#)

[▶](#)

[◀](#)

[▶](#)

[Back](#)

[Close](#)

[Full Screen / Esc](#)

[Printer-friendly Version](#)

[Interactive Discussion](#)

A new approach to accurate validation

C. Sun et al.

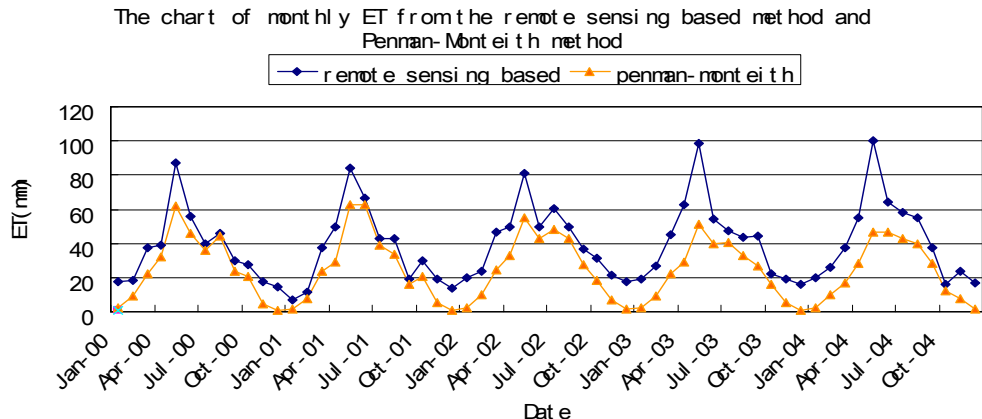


Fig. 5. The monthly ET result from the remote sensing based method and penman-monteithmethod from the year of 2000 to 2004.

[Title Page](#)[Abstract](#)[Introduction](#)[Conclusions](#)[References](#)[Tables](#)[Figures](#)[◀](#)[▶](#)[◀](#)[▶](#)[Back](#)[Close](#)[Full Screen / Esc](#)[Printer-friendly Version](#)[Interactive Discussion](#)

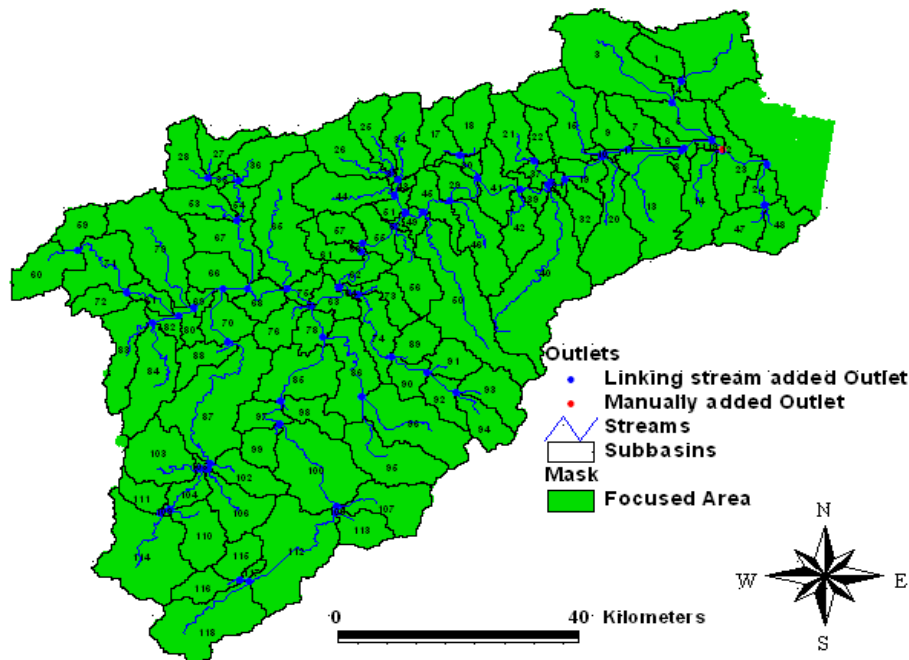


Fig. 6. The map of the subbasin produced by SWAT.

A new approach to accurate validation

C. Sun et al.

[Title Page](#)

[Abstract](#)

[Introduction](#)

[Conclusions](#)

[References](#)

[Tables](#)

[Figures](#)

[◀](#)

[▶](#)

[◀](#)

[▶](#)

[Back](#)

[Close](#)

[Full Screen / Esc](#)

[Printer-friendly Version](#)

[Interactive Discussion](#)

The chart of yield from the remote sensing based & Penman-Monteith method with SWAT

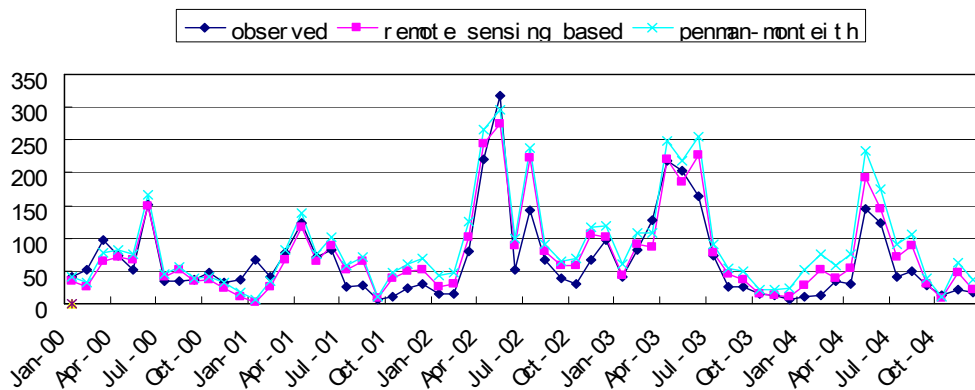


Fig. 7. The monthly runoff simulated from the remote sensing based method, penman-monteith method with SWAT and the observed runoff from the year of 2000 to 2004.

A new approach to accurate validation

C. Sun et al.

[Title Page](#)

[Abstract](#)

[Introduction](#)

[Conclusions](#)

[References](#)

[Tables](#)

[Figures](#)

[◀](#)

[▶](#)

[◀](#)

[▶](#)

[Back](#)

[Close](#)

[Full Screen / Esc](#)

[Printer-friendly Version](#)

[Interactive Discussion](#)



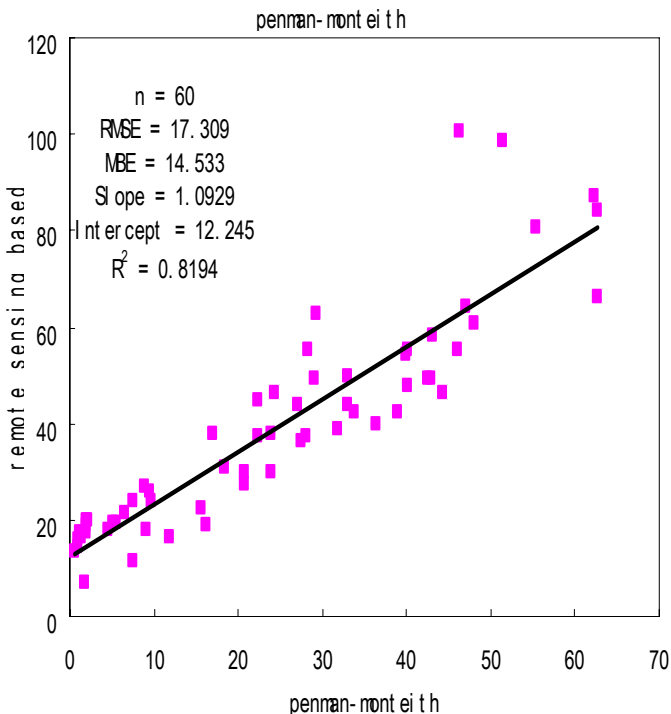


Fig. 8. The monthly ET result b between the two methods: Penman-monteith, and the Remote sensing based result.

A new approach to accurate validation

C. Sun et al.

[Title Page](#)

[Abstract](#)

[Introduction](#)

[Conclusions](#)

[References](#)

[Tables](#)

[Figures](#)

[◀](#)

[▶](#)

[◀](#)

[▶](#)

[Back](#)

[Close](#)

[Full Screen / Esc](#)

[Printer-friendly Version](#)

[Interactive Discussion](#)



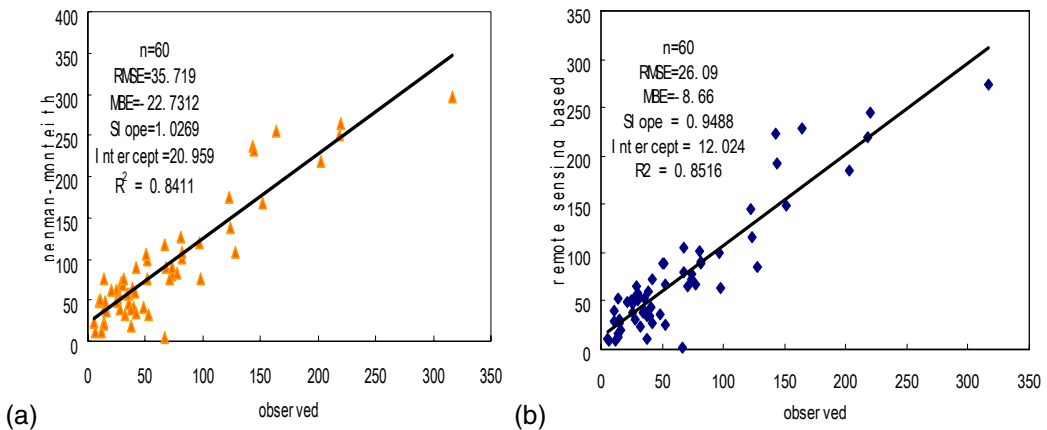


Fig. 9. The monthly runoff simulated from the remote sensing based method and Penman-monteith method with SWAT versus the observed runoff data. **(a)** is the simulated runoff with Penman-monteith model versus the observed runoff. **(b)** is the simulated runoff with remote sensing based model versus the observed runoff.

A new approach to accurate validation

C. Sun et al.

[Title Page](#)

[Abstract](#)

[Introduction](#)

[Conclusions](#)

[References](#)

[Tables](#)

[Figures](#)

[◀](#)

[▶](#)

[◀](#)

[▶](#)

[Back](#)

[Close](#)

[Full Screen / Esc](#)

[Printer-friendly Version](#)

[Interactive Discussion](#)